Volume 4
Number 7
July 2025
Pages 983–1132

Environmental Science Advances

rsc.li/esadvances

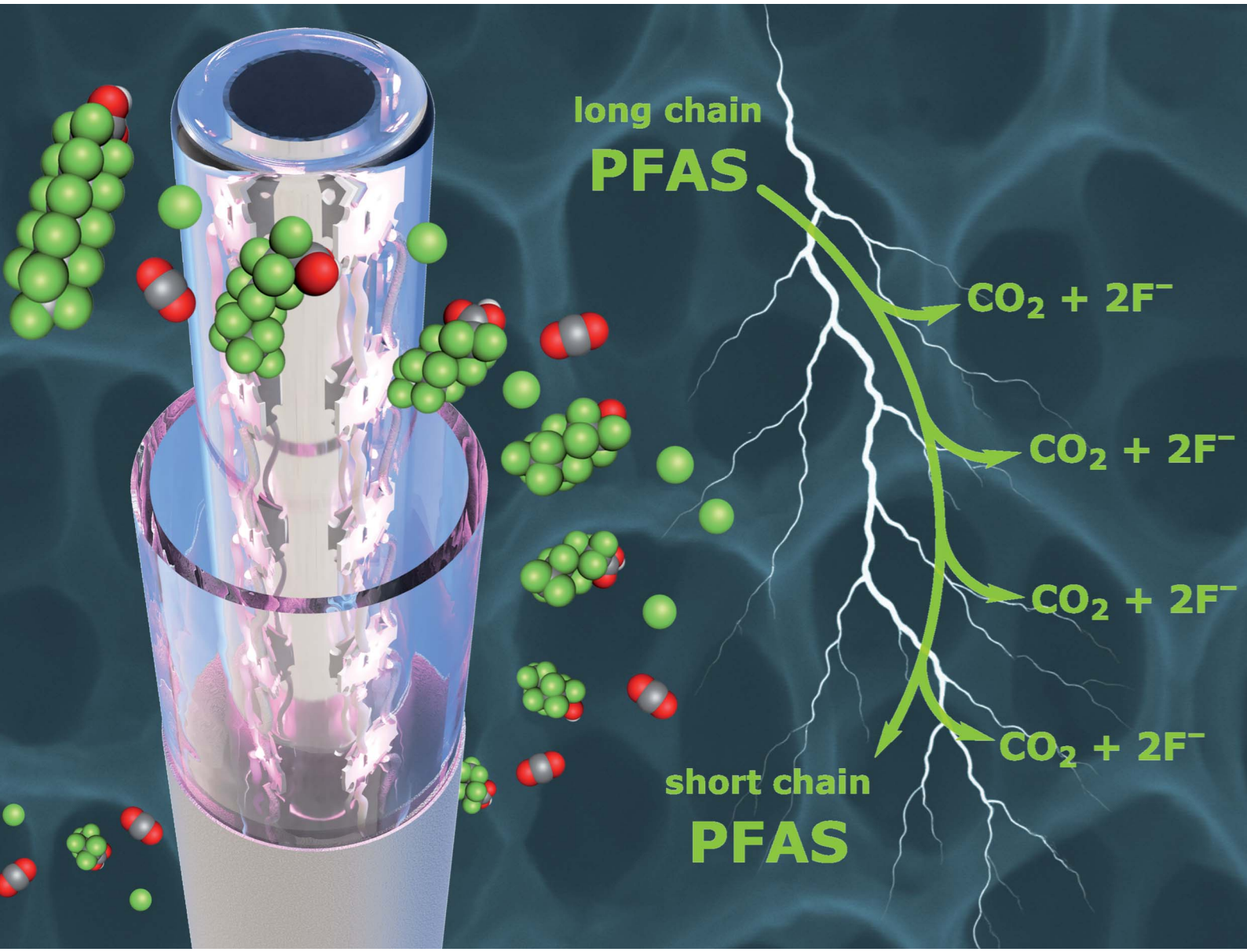

ISSN 2754-7000

ROYAL SOCIETY OF CHEMISTRY

PAPER

J. Scott McIndoe *et al.*

Bias enhanced electro-photocatalysis on TiO_2 nanoporous materials for decomposition of forever chemicals in saltwater

Environmental Science Advances

PAPER

View Article Online
View Journal | View Issue

Cite this: *Environ. Sci.: Adv.*, 2025, **4**, 1024

Bias enhanced electro-photocatalysis on TiO_2 nanoporous materials for decomposition of forever chemicals in saltwater†

Sapanbir S. Thind, [ab] Bobby A. Ryane,[a] John. B. Hayden,[b] Ian Chagunda, [a] Mathias Paul[a] and J. Scott McIndoe *[a]

In this study, a TiO_2-based bias-enhanced photocatalytic system was prepared with the aim of achieving high photocatalytic activity in deionized as well as in saltwater systems. Highly ordered TiO_2 nanoporous materials were fabricated *via* a double-anodization method. A potential bias was applied that suppresses electron–hole recombination and deters interference from the ions present in the solution while minimizing electrochemical reactions. Photodegradation reactions involving Rhodamine B (RhB) were conducted to evaluate the efficacy of the nanomaterials with and without the applied bias. Our experimental results revealed that the synthesized TiO_2 nanomaterials possessed high photochemical activity under UVA light, substantially enhanced with the applied bias. A very significant enhancement was observed when the Bias Enhanced Electrolytic Photocatalysis (BEEP) system was used in saline solutions. Higher photocatalytic efficiency was achieved with the increase in the salinity level in the reaction mixture. These bias-enhanced nanomaterials were successfully tested for the degradation of per- and polyfluorinated substances (PFAS), recognized as a significant threat to the environment and human health. The results indicated that the presented technology could eliminate a wide range of fluorinated molecules. The simplicity, efficacy and scalability of the new BEEP approach described in this study make use of the TiO_2-based advanced oxidation process (AOP) possible in designing high-performance water purification technologies applicable to fresh and salt water.

Received 19th December 2024
Accepted 28th February 2025

DOI: 10.1039/d4va00423j

rsc.li/esadvances

Environmental significance

Accumulation of per- and poly-fluoroalkyl substances (PFAS) in the environment has gathered increasing attention from the scientific community because of their potential adverse effects on the ecosystem and humans. Traditional methods such as electrolysis and supercritical water treatment are very energy-inefficient and expensive. With 96% of Earth's water being saltwater or brackish, an energy-efficient treatment method that can operate across all levels of salinity is needed to support the natural processes and reduce aquatic concentrations of these "forever chemicals". Here we report the development of an advanced photocatalytic system for energy-efficient water treatment applications. To circumvent the issue of ionic interference during photocatalysis a potential bias was applied which significantly enhanced the photocatalytic activity in the saline water.

Introduction

Fast urbanization and increased industrialization are putting enormous stress on our water environment. Polluted water is of great concern to the aquatic biome, humanity, and climate and negatively affects the ecosystem.[1,2] The World Economic Forum has listed the degradation of freshwater resources among the top ten biggest global risks for the past decade. The world's water resources have become contaminated, primarily by chemicals and microorganisms, from either point or non-point sources of pollution, which interfere with the beneficial use of the water or with the natural functioning of ecosystems. Up to 5.5 billion people worldwide could be exposed to polluted water by 2100, a modelling study has found.[3]

Some of the most challenging pollutants that society faces are per- and polyfluoroalkyl substances (PFAS), which form a huge group of diverse anthropogenic chemicals. The unique properties of PFAS, for instance, water-, stain-, and oil repellency and their high chemical stability, led to widespread use in areas as diverse as fire-fighting foams and upholstery coatings. The PFAS are highly stable due to the strong C–F bond which resulted in their worldwide distribution. Perfluoroalkyl acids (PFAAs) in particular were detected throughout the water cycle, plants, and animals of a region including humans, air, indoor

[a]*Department of Chemistry, University of Victoria, 3800 Finnerty Road, Victoria, BC, V8P 5C2, Canada. E-mail: mcindoe@uvic.ca*

[b]*Waterdrape LLC, Paradise Valley, Arizona, USA*

† Electronic supplementary information (ESI) available. See DOI: https://doi.org/10.1039/d4va00423j

environments, and soils.[4] Today, selected PFAAs fall under global regulations to restrict their use due to high persistence, bioaccumulation potential, and adverse health effects. The main technologies currently in use for PFAS removal, are supercritical water treatment,[5,6] foam fractionation,[7] and electrolysis.[8] These technologies usually operate under extreme conditions and consume high energy.

Heterogeneous photocatalysis (HPC) based Advanced Oxidation Process (AOP) is an eco-friendly technique for purifying water from organic and biological pollutants in environmental systems.[9,10] Upon light irradiation, the HPC process harnesses photon energy resulting in photoexcitation of the electron from the valence band to the conduction band causing an electron–hole pair separation (e^-/h^+) and activation of surface redox reactions. The reactive oxygen species resulting from the redox reactions on the surface of the photocatalyst play a vital role in converting adsorbed organic/inorganic pollutants into less harmful compounds.[11,12] Light harvesting, photogenerated charge separation and surface reactivity play a very significant role in the performance of photocatalysts.

TiO_2 as a photocatalyst is considered one of the best materials for the degradation of hazardous pollutants due to its strong oxidizing power, high photocatalytic activity, chemical and biological stability, relatively low cost, nontoxicity, and long-term photostability.[13,14] TiO_2 with different morphologies such as nanospheres,[15] nanotubes,[16] nanorods,[17] nanofibers,[18] nanowires[19] have been reported for the removal of pollutants from water. In addition, TiO_2 surfaces become super hydrophilic with a contact angle of less than 5° under UV-light irradiation, due to chemical conformation changes on the surface.[20] Among the current methods, different forms of TiO_2 have been shown to break down perfluorooctanoic acid (PFOA), but it has been mostly focused on TiO_2 particles.[21,22] Where TiO_2 particles show some promise, they still leave the issue of low removal rates of PFOA and PFOS and require the removal of the TiO_2 particles from the water source. TiO_2 modified with different particles have also been investigated for the photodegradation of PFOAs, such as Pb,[23] Bi,[22] In,[24] and Fe.[25] TiO_2 array sheets have not yet been investigated for PFAS degradation.[26,27]

While pilot-scale HPC and TiO_2-based photocatalysts have explored photocatalytic system scalability, their practical implementation is restricted for various reasons. These include low efficiencies, complicated photoreactor designs, high operation and synthesis costs, photocatalyst poisoning, and fast electron–hole recombination.[28–31] In the past four decades, a variety of strategies have been proposed to adjust the physical and chemical properties of semiconductor photocatalysts to effectively improve the scope of light absorption, reduce the recombination of photogenerated charge carriers, and accelerate surface redox reactions. Anionic and cationic doping,[32–35] composite materials synthesis,[36,37] and nanomaterials with complicated morphologies[38,39] are stuck at the proof-of-concept level. Although a lot of work has been done on basic photocatalytic research, there is still a gap between laboratory and industrial applications.[29]

Accordingly, we have developed a technology we call Bias Enhanced Electrolytic Photocatalysis (BEEP), where a potential bias to the anode is applied to boost the redox reactions on the surface of TiO_2. Applying potential bias on the TiO_2 can seize photo-generated electrons from the conduction band. The electric potential enhances this system whether in saline water or non-saline water. The enhancement can be attributed to two factors. (1) band bending which leads to helping oriented transfer of the photogenerated electrons, thus a reduction of electron–hole recombination takes place as the positive voltage on the anode keeps the electron longer in the conduction band, thus giving the hole enough time to react with the water molecules to form hydroxyl radicals that help in oxidizing the pollutant molecules.[40] (2) A positive charge on the anode (TiO_2) helps to keep an electric charge on the photocatalyst's surface, repulsing the unwanted inorganic cations. Accordingly, less interference by these ions on the photocatalytic activity of the photocatalyst is observed. For TiO_2 semiconductor materials, the applied potential bias collects the electrons made available by the interfacial photocatalytic reactions. Maximum (100%) photogenerated-electron collection efficiency can be achieved only when the applied potential bias is sufficiently positive.[41] We tested the developed BEEP technology against a typical photocatalytic reactor and a significant increase in the photocatalytic reactivity was observed in distilled water as well as in seawater level salinity. The result is significant because it means that the technology can be effectively deployed for degrading pollutants in distilled water, brackish water, and seawater with only minor modifications to the reactor. We also successfully tested BEEP with some of the most challenging pollutants, namely per- and polyfluoroalkyl substances (PFAS). The results show that BEEP is capable of destroying various PFAS. BEEP is energy efficient compared to other processes currently used to eliminate PFAS from water such as supercritical water treatment, foam fractionation, and electrolysis. Defluorination of the PFAS chains can also be achieved.

Experimental

Materials

Titanium metal tubes were purchased from Ticon Industries (Leander, Texas, USA). Hydrochloric acid (38%), ethylene glycol, Rhodamine B, acetone, ammonium fluoride, perfluorononanoic acid and perfluorotetradecanoic acid were purchased from Sigma Aldrich and used as is. To check the photocatalytic removal of PFAS mixtures (Method 537 and 537.1 M), solutions were obtained from Weck Laboratories Inc. California.

Fabrication and modification of nanoporous TiO_2

The highly ordered nanoporous TiO_2 was grown using an anodization process in a one-compartment two-electrode cell that contained ethylene glycol + 0.3 wt% NH_4F + 2 wt% H_2O, with a Ti tube as the anode, and a titanium mesh as the cathode. Briefly, the Ti metal tube was initially sonicated in acetone for 15 min, after which it was etched in 18% HCl at 85 °C for

10 min. Subsequently, the etched Ti was anodized at 50 V over 5 h, after which the rough as-grown nanoporous TiO_2 layer was removed by applying masking tape. The same Ti then underwent a second-step anodization at 50 V for 15 min to obtain a uniform nanoporous TiO_2 structure. The plates were annealed at 450 °C for 3 h to obtain an anatase crystal structure.

Characterization of the synthesized nanoporous TiO_2

The synthesized nanoporous TiO_2 was characterized by energy-dispersive X-ray spectroscopy (EDX), and scanning electron microscopy (SEM, Hitachi-S400). X-ray diffraction (XRD) measurements were done on a PANalytical Empyrean system using a Cu (Kα, 1.5406 Å). An LED assembly containing 365 nm UVA LEDs was employed to evaluate the prepared nanomaterial's photocatalytic activity. The LEDs were purchased from Mouser USA (Mouser #:416-LST101G01UV01).

Photocatalytic reactor

The photoreactor consists of a titanium tube (Fig. 1A) with TiO_2 nanoporous material grown on the inner surface. A stainless-steel pipe runs through the middle of the titanium tube and connects the pump at the bottom to the sprayer at the top. Water is sprayed vigorously onto the TiO_2 surface, scrubbing the air. The water runs down as a thin film on the TiO_2 nanoporous material inside the titanium tube. The UVA-LED assembly (fifteen 365 nm UVA LEDs secured in a glass tube wrapped around the stainless-steel pipe) irradiates the inner surface of the titanium tube as shown in Fig. 1B. The treated water falls into the reservoir from which it can be recycled for further treatment. The volume of this reservoir is 2 L and the flow rate during the experimentation was approximately 3 L min^{-1}.

Photocatalytic activity measurements

The photocatalytic activity of synthesized nanoporous TiO_2 was evaluated by measuring the photocatalytic degradation of Rhodamine B (RhB) under different conditions. A 10 μM solution was prepared in tap water. The reaction mixture was stirred for 30 min in the absence of light to obtain a homogeneous dissolution of dye in the water and achieve an adsorption–desorption equilibrium. The UV intensity on the TiO_2 surface was measured to be around 8000 mW cm^{-2}. DC electricity for the LED assembly was maintained at approximately 21 watts (2.0 amps constant current with a forward voltage of ~10.7 volts). Samples were collected from the reaction mixture at regular intervals. The samples were used to measure the degradation of Rhodamine B using a UV-vis spectrometer (ASEQ instruments LR1-B). After taking the reading the solution was added back to the reactor. For bias-enhanced electrolytic photocatalysis, 2 V was applied between TiO_2 coated metal tube and the stainless-steel chalice which contains the solution. When the pump is off there is no water flow in the system and thus no circuit is established between the anode and cathode as they are separated by a silicone ring. When the pump is on, the water gets sprayed on the TiO_2 and falls back into the chalice resulting in establishing an electrical connection through the solution between the anode and the cathode.

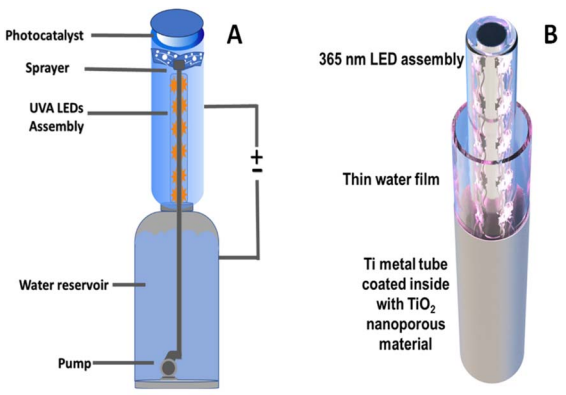

Fig. 1 (A) Design of the photoreactor. (B) Inside view of the reactor showing design of the LED assembly.

PFTeDA/PFNA degradation analysis

Samples were taken from the reactor (Fig. 1), and data was collected by a Waters (Milford, USA) Synapt G2-Si mass spectrometer and analyzed using Waters MassLynx V4.2 software. The Synapt was operated in negative ion mode. Parameters used were: capillary voltage 2.50 kV, source temperature 115 °C, desolvation temperature 220 °C, sampling cone 20, source offset 0, desolvation gas flow rate 150 L h^{-1}, cone gas flow 50 L h^{-1}, mass range m/z 50–800, and scan duration 1 s (Fig. S6†).

Electrochemical testing

The electrochemical testing was performed using linear sweep voltammetry on a Gamry Instrument Interface 1010 E, using Gamry Framework Data Acquisition V. 7.10.3 software. A Ag/AgCl reference electrode was placed at the top of the BEEP system near the top of the anode and UV lights. The data collection was performed at a scan rate of 10 mV s^{-1}, step size of 2 mV, with an initial volt of −0.215 V, and final volts of 3 V. The experiment used the BEEP system shown in Fig. 1A.

Results and discussion

The SEM image (Fig. 2A) of the highly ordered nanoporous material fabricated on the Ti substrate by the anodization method revealed that the diameter of the nanopores was ~150 nm and that the nanopore consisted of several smaller nanopores. The diffraction peaks (Fig. 2B) were attributed to the tetragonal anatase TiO_2,[16] which confirmed the anatase phase after heating at 450 °C for 3 h.[18] The peaks marked with asterisks are derived from the Ti substrate. Strong oxygen and titanium peaks were observed in the EDS (Fig. 2C), which confirmed the formation of the TiO_2 nanoporous arrays. We tested the BEEP photoreactor under various conditions. The degradation reaction of RhB under UVA light (365 nm) irradiation was used to evaluate the photocatalytic activity. It was compared with the bias-applied degradation and the photocatalyst with bias enhancement (BEEP). Fig. 2D presents the disappearance of RhB under photooxidation conditions.

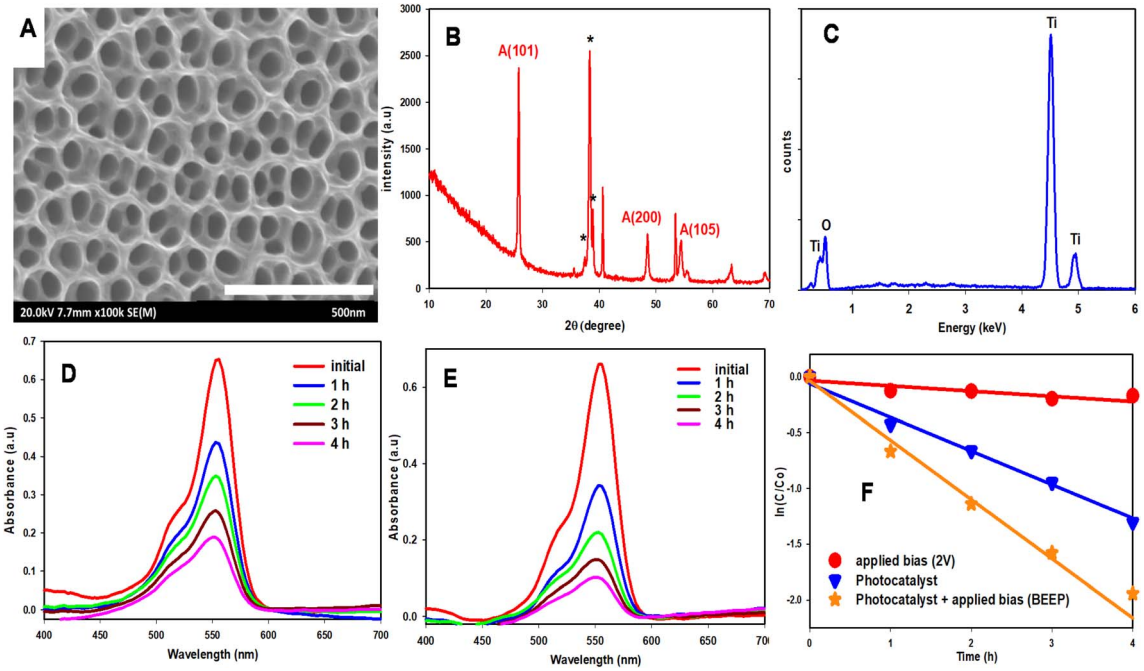

Fig. 2 (A) SEM image of prepared TiO_2 nanoporous materials. (B) XRD spectra of TiO_2. (C) EDX spectra. Scanning kinetic curves for (D) photo- (E) BEEP oxidation of Rhodamine B in distilled water on TiO_2 nanoporous material. (F) The relationship between $\ln(C/C_0)$ and time.

Substantial removal of the organic dye was noted and within four hours of testing, the dye concentration was reduced by approximately 65%. In our next experiment, BEEP technology was engaged where the UVA light was turned on and a potential bias of 2 V was applied to the TiO_2 nanomaterials. As seen in Fig. 2E the rate of photocatalytic removal of RhB with BEEP was faster compared to when only the photocatalyst was applied. The kinetics of these reactions are presented in Fig. 2F, revealing that a ~50% enhancement in the photocatalytic activity was observed when BEEP was used. Even when no electrolyte is present in the solution, applying 2 V on the anode helps in the reduction of electron–hole recombination and improves the redox kinetics at the surface thus improving the overall photocatalytic activity of the photocatalytic system. TiO_2 is a wide bandgap semiconductor (3.2 eV)[42] and cannot be used as an electrocatalyst on its own. Fig. S1† presents an attempt to use our reactor where TiO_2 is behaving as an electrocatalyst with an applied voltage of 2 V. During this experiment, there was no UVA irradiation on the TiO_2. As expected, little electrocatalytic removal of RhB was observed and after four hours only 18 percent was oxidized. There was no electrolyte in the solution and the current was in microamperes.

Photocatalysts have been studied in the presence of different inorganic salts, and it is well-established that the photocatalytic efficiency significantly decreases due to the ions in the solution.[43,44] The vast majority of water on the earth's surface, over 96 percent, is saline water in the oceans. Most of the pollutants released by different industries ultimately find their way into the oceans and there is no efficient way of getting rid of these pollutants. The salinity of oceans is usually around 35 000 ppm, which badly compromises the efficiency of a typical photocatalytic reactor. Thus, there is an urgent need to develop new technologies for the treatment of saline wastewater. To test the BEEP technology and to understand the effect of salinity, we performed experiments on solutions with different salinity. Fig. 3A and B represent photocatalytic experiments conducted with 35 000 ppm salt water without and with BEEP engaged respectively. The results indicate that as expected, the photocatalysis was severely hindered by the presence of salt in the water and the reaction was much slower compared to the photocatalysis in fresh water. Although there is a large amount of salt in the water that contributes as an electrolyte, the electrocatalysis experiment where 2 V was applied without the UVA irradiation on the photocatalyst did not increase the rate of reaction (Fig. S2†). This lack of activity is because 2 V is not enough of a potential bias to activate the TiO_2 as an electrocatalyst in such conditions. When BEEP was engaged, a faster reaction was observed and within the first hour, most of the stand-in organic pollutant (RhB) was oxidized. The inset image in Fig. 3B shows that nearly all the colour of the dye disappeared within one hour and the two-hour sample was clear with no trace of the dye molecule shown in the UV-Vis spectra. Reaction rates obtained from these results revealed that when the BEEP reactor was used for the treatment of RhB in 35 000 ppm water, it showed approximately 16 times faster degradation of RhB as compared to just the photocatalyst without engaging BEEP (Fig. S3†). This result demonstrates that the synergistic application of applied bias greatly boosts the photocatalytic properties of the system due to the repulsion of unwanted inorganic cations on the surface of the anode, leading to less interference on the photocatalytic activity of the photocatalyst, in addition to lower recombination.

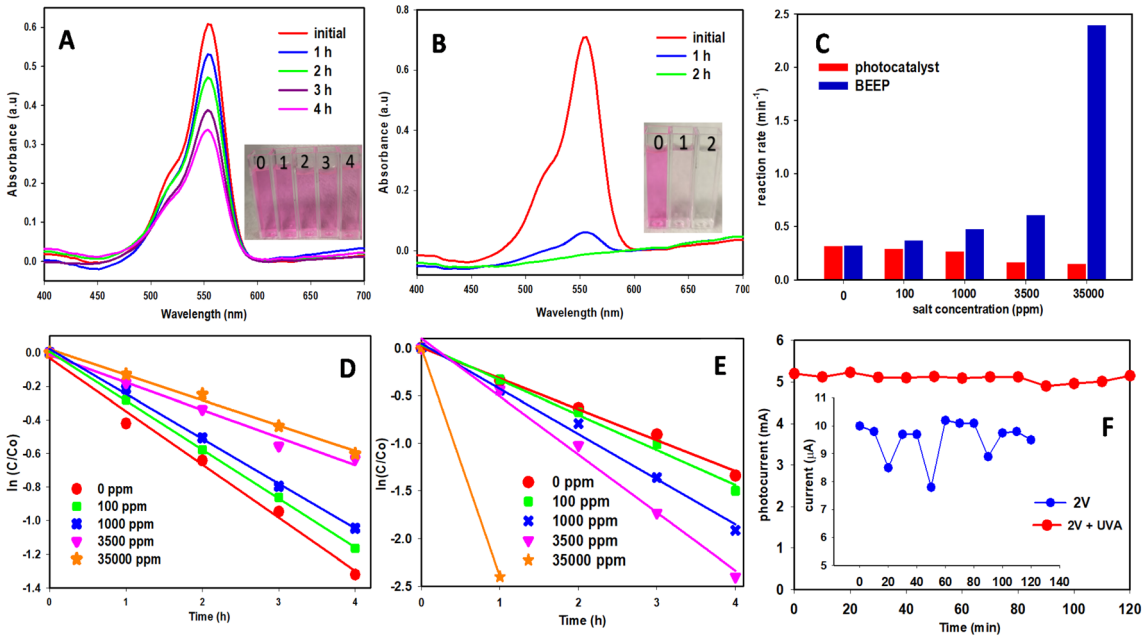

Fig. 3 Scanning kinetic curves for (A) photo- (B) photoelectrochemical (BEEP) oxidation of Rhodamine B in 35 000 ppm saltwater on TiO_2 nanoporous material. (C) The rate constants for the photocatalytic oxidation of RhB at various salinity levels during photocatalytic (red) and BEEP (blue). The relationship between $\ln(C/C_0)$ at various salinity levels for experiments performed with (D) photocatalysis only (E) BEEP. (F) Current and photocurrent at 3500 ppm salinity.

To further study the effect of the salt concentration on the photocatalysis, we altered the experimental conditions. Fig. 3C shows the effect of different salinity levels on the performance of photocatalysis and BEEP. When just photocatalysis was used and no potential bias was applied, with an increase in the salt concentration, the photocatalytic activity of the TiO_2 decreased. An 8% decrease in the activity was observed when the salinity level of the solution was increased from 0 to 100 ppm. With further increases in the salinity, 16%, 48%, and 52% decreases in reaction rate were observed for the 1000, 3500, and 35 000 ppm solutions respectively. In contrast, when BEEP was engaged (*i.e.* the photocatalyst was irradiated with UVA and a 2 V potential bias was applied), instead of a decrease a significant increase in the activity was observed, and 113, 146, 187, and 740% increases in the photocatalytic activity was observed for 100, 1000, 3500 and 35 000 ppm solution. The kinetic curves for these experiments are presented in Fig. 3D and E. These results signify that BEEP is not only advantageous in freshwater treatment systems but is transformative in a saline environment. BEEP not only keeps the photocatalyst engaged but also significantly enhances its activity. This enhancement in activity can be attributed to the higher photocurrent observed when the bias is applied in the presence of UVA (Fig. 3F). The effect of applied bias on the photocurrent in 3500 and 35 000 ppm salt solution is present in Table S1 and S2† respectively.

The effect of applied bias in pure water (0 ppm salt) and salt water (35 000 ppm) on the photocurrent is represented in a Linear Sweep Voltammetry (LSV) graph which is an electrochemical technique that measures the current at an electrode while linearly increasing the potential between the electrode and a reference electrode. The results are presented in Fig. S4.† From 0 V to 2.25 V a linear response is observed, indicating that no water splitting is taking place at this potential range. After 2.5 V exponential growth is seen in the current which presents the water-splitting. Thus, 2 V was used to operate BEEP as it has a high enough positive bias to eliminate most of the electron–hole recombination without causing water splitting. Water-splitting negatively affects the photocatalysis.

PFAS have been used as water repellants on fabrics and household textiles and non-stick coatings on and in food packaging and cookware for decades.[4,45,46] These PFAS are now being linked to a wide range of health issues.[47–51] Eventually, the PFAS are solubilized in aqueous landfill leachate. Removal of aqueous PFAS typically requires more energy- and resource-intense methods such as reverse osmosis, nano-filtration, ion exchange processes, supercritical conditions or sorptive filtration using granular activated carbon or biochar.[52–54] Heterogeneous photocatalytic oxidation has emerged as an effective alternative technique for the degradation of PFAS.[55,56] Most studies have been done with slurry reactors and UVC lights and photocatalysts like In_2O_3 or Ga_2O_3, and degradation of PFAS has been demonstrated.[55] However, these photocatalysts are very expensive to utilize in industrial applications.

For experimentation, PFAS samples were obtained from Weck Laboratories Inc. California, USA, and were used as received for the BEEP-based photocatalytic redox studies. Two different types of methods/solutions were obtained for this study. EPA 537.1, which is commonly used for drinking water testing, and EPA 537M, which is for non-potable water and soil/

solids.[57,58] In the first experiment, a solution containing 42 PFAS with different functional groups and different chain lengths was used to evaluate the efficiency of the BEEP photocatalytic reactor toward the removal of these PFAS. The results are shown in Fig. 4. Fig. 4A shows the amount of different perfluorocarboxylic acids (PFCAs) chains in the initial sample (red) and after 24 h BEEP treatment (orange). It can be concluded that complete removal of perfluorooctadecanoic acid [PFODA ($C_{17}F_{35}COOH$)], perfluorohexadecanoic acid [PFHxA $C_{15}F_{31}COOH$], perfluorotetradecanoic acid [PFTeDA/PFTDA ($C_{13}F_{27}COOH$)], perfluorotridecanoic acid [PFTrDA ($C_{12}F_{25}COOH$)] were achieved. All these analytes were undetectable by the LC/MS/MS after 24 h experimental run. It is to be noted that all these PFCA chains were the longest fluorocarbon chains present in the solution. This shows that longer molecules of the PFAS are more susceptible to photocatalytic elimination. In the case of PFCAs, with an increase in the number of carbon atoms in the molecule, their water solubility decreases. The negative charge of the carboxylic acid group on the PFCA is attracted to the positive charge applied to the TiO_2 nanoporous material. These hydrophobic molecules have the tendency to easily come out of water and adsorb onto the TiO_2 surface where they react with hydroxyl radicals and holes, which are highly oxidizing in nature resulting in the breaking of C–C bonds in the PFAS. For the PFCA chains with 12, 11, 10, 9, and 8 carbon atoms, approximately 97%, 95%, 85%, 56%, and 26% decreases in PFCA were observed, respectively. The PFCA chains with a lower number of carbon atoms showed higher accumulation after 24 h of the photocatalytic redox process. For example, for perfluorooctanoic acid [PFOA $C_7F_{15}COOH$ (C8)], the amount present in the 24 h sample was 169% more than the amount present in the initial sample. All these results indicate that the longer chain molecules are getting decomposed on the surface of the TiO_2 photocatalyst resulting in the formation of PFAS with smaller carbon chains. The overall mechanism for this fragmentation can be provided as follows with an example of perfluorododecanoic acid [PFDoA (C12)].[22,55] In the first step, the PFCA ions are adsorbed on the surface of the TiO_2 nanoporous materials and get oxidized and produce a radical species. This radical molecule undergoes a decarboxylation reaction to form CO_2 and a very unstable decarboxylated carbon chain that immediately reacts with a water molecule to produce H^+ and an OH^- containing carbon chain. Further reactions form PFCAs containing one less carbon atom than the parent molecule. From the conduction band, excited e^- on the surface of the photocatalyst reacts with adsorbed water to form hydrated electrons (e_{aq}^-). PFAS molecules adsorbed on the catalyst surface can be attacked by the e_{aq}^- and degraded into shorter-chain compounds. These reactions are presented in detail below.[53]

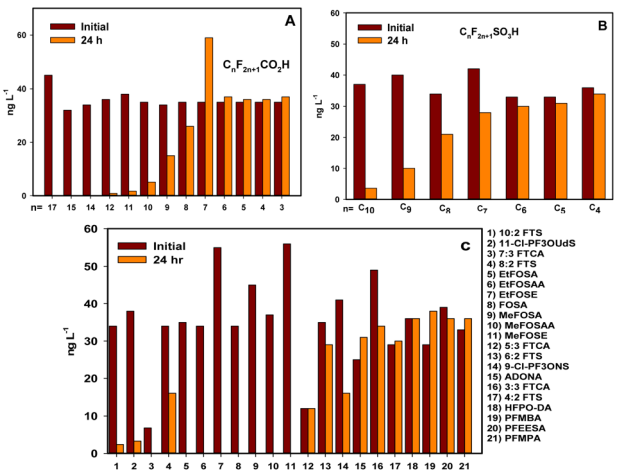

Fig. 4 537 M testing with 42 analytes. Effect of BEEP photocatalytic redox reaction on the concentration of (A) PFCAs, (B) PFSAs and (C) various other PFAS.

$$TiO_2 + h\nu \rightarrow TiO_2\,(h^+ + e_{aq}^-) \quad (1)$$

$$H_2O + h^+ \rightarrow H^+ + OH^\bullet \quad (2)$$

Decomposition by h^+

$$C_{11}F_{23}COO^- + h^+ \rightarrow C_{12}F_{23}COO^\bullet \quad (3)$$

$$C_{11}F_{23}COO^\bullet \rightarrow C_{11}F_{23}^\bullet + CO_2 \quad (4)$$

$$C_{11}F_{23}^\bullet + H_2O \rightarrow C_{11}F_{23}OH + H^+ \quad (5)$$

$$C_{11}F_{23}OH \rightarrow C_{10}F_{21}COF + H^+ + F^- \quad (6)$$

$$C_{10}F_{21}COF + H_2O \rightarrow C_{10}F_{21}COO^- + 2H^+ + F^- \quad (7)$$

Decomposition by e^-

$$C_{11}F_{23}COOH + e_{aq}^- \rightarrow C_{11}F_{22}COOH^\bullet + F^- \quad (8)$$

$$C_{11}F_{22}COOH^\bullet + H_2O \rightarrow C_{11}F_{22}HCOOH + OH^\bullet \quad (9)$$

$$C_{11}F_{22}HCOOH + e_{aq}^- \rightarrow C_{11}F_{21}HCOOH^\bullet + F^- \quad (10)$$

$$C_{11}F_{21}HCOOH^\bullet + H_2O \rightarrow C_{11}F_{21}H_2COOH + OH^\bullet \quad (11)$$

$$C_{11}F_{21}H_2COOH \rightarrow C_{10}F_{21}^\bullet + :CH_2 + COOH^\bullet \quad (12)$$

$$C_{10}F_{21}^\bullet + COOH^\bullet \rightarrow C_{10}F_{21}COOH \quad (13)$$

$$:CH_2 + H^\bullet \rightarrow {}^\bullet CH_3 \quad (14)$$

With time, larger molecules are broken down resulting in the formation of smaller chains showing a cascade effect on their concentration. This conclusion can be further supported by the results in Fig. 4B, which shows the photocatalytic removal of different sulfonic acid chains present in the solution. Perfluorodecane sulfonic acid [PFDS (C10)] is the longest molecule present in this group and showed 90% removal in 24 h. The shorter fluoride-containing carbon chains, 9, 8, and 7, have a decrease of 75%, 38%, and 33% in the 24 h, respectively. As photocatalytic redox reactions take place on the surface, the molecules get broken down further and further leading to the

formation of shorter-chain PFAS. As this test solution had 42 different PFAS, Fig. 4C presents the effect of BEEP redox on the concentration of PFAS containing other functional groups proving that irrespective of the functional groups/molecular structure, BEEP can effectively and efficiently destroy them. Complete removal of PFAS with sulfonamide-containing groups was observed. *N*-Methyl perfluorooctane sulfonamide [MeFOSA], *N*-methyl perfluoroctane sulfonamide [MeFOSA], *N*-methyl perfluorooctane sulfonamido acetic acid [MeFOSAA], *N*-ethyl perfluorooctane sulfonamide [EtFOSA], *N*-ethyl perfluoroctane sulfonamide [EtFOSA], and *N*-ethyl perfluorooctane sulfonamido acetic acid [EtFOSAA] were all undetectable after 24 h of treatment under BEEP conditions.

To repeat the result and to limit the interference from so many additional PFAS analytes in the sample, another BEEP redox experimentation was performed, but this time only 18 analytes were present in the solution and the 48 h photocatalytic redox results for these analytes are shown in Fig. S5.† The results follow the same trend as observed in the previous experiment and longer-chain PFCAs showed faster removal rates compared to the smaller carbon chains. An increase in the amount of smaller carbon chain analytes was again observed. After the 48 h photocatalytic redox by BEEP, perfluoropentanoic acid [PFPeA (C5)], and perfluorobutanoic acid [PFBA (C4)] were detected in very small amount. These analytes were not present in the initial solution, again backing the proposition that the bigger chains are getting broken into smaller chains.

Single analyte experiments were performed on perfluorotetradecanoic acid [PFTeDA (C14)] and heptadecafluorononanoic acid [PFNA (C9)]. To utilize the true benefits of BEEP, an experiment using PFTeDA was performed with 100 ppm salt concentration. An intense molecular ion peak at *m*/*z* 712.953 and a decarboxylated molecular ion peak at *m*/*z* 668.957 was observed. A consistent decrease in the PFTDA was observed during the experiment and after 24 h of BEEP treatment, most of the PFTeDA was gone and several product peaks were observed. Some of these peaks can be assigned to smaller PFCA molecules like $[C_8F_{17}]^-$ and $[C_6F_{13}]^-$ at *m*/*z* 418.976 and 318.982 respectively (Fig. S6C;† these entities are decarboxylated and unsaturated).[59] Fig. 5A shows the mass spectrum of $[C_{13}F_{27}CO_2]^-$ and $[C_{13}F_{27}]^-$ obtained for all the samples taken during the experimentation. A gradual decrease in the concentration of PFTeDA was observed and within 12 h, the concentration was below the detection limit of the mass spectrometer as no peaks were observed at *m*/*z* 668.957 and *m*/*z* 712.953. This observation suggests that in the beginning, the PFTeDA molecule with 14 carbon atoms is degraded by removing a CF_2 unit, which results in creating molecules with 13 carbon atoms. The corresponding $[C_{12}F_{23}CO_2]^-$ ions appear at *m*/*z* 662.963 (Fig. S6†). Due to the highly oxidizing capabilities of BEEP, this byproduct further breaks down into smaller molecules resulting in its disappearance from the 4 h and subsequent samples. There is nothing observable in the 24 h sample as this product further gets broken down to low molecular weight products.

Heptadecafluorononanoic acid was used to verify that BEEP could break down smaller chain PFAS, since it was observed in Fig. 4 that there was an increase in smaller alkyl chains. To

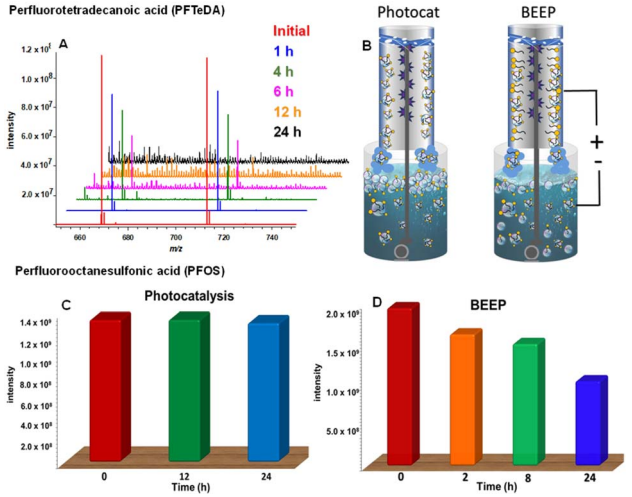

Fig. 5 (A) MS spectra during the BEEP redox of PFTeDA. (B) Possible reaction mechanism depiction during the redox breakdown of PFAS on BEEP. MS spectra intensities for PFOS molecular ion during the photocatalysis (C), and BEEP (D).

increase the reaction rate, 4.0 V and pH 2.5 were used. As can be seen in Fig. S7,† there was a decrease in the C9 chain, leading to a rise and fall in the smaller chains. After 24 h very small amounts of $[C_4F_9]^-$ (*m*/*z* 218.95) and $[C_5F_{11}]^-$ (*m*/*z* 268.95) were seen, and then after 48 h no PFAS were observed. The energy efficiency of BEEP was compared to a similar study[60] and is reported in Table S3.†

Perfluorooctanesulfonic acid (PFOS) is a compound with a chain length containing eight perfluorinated carbon atoms (C8) bonded to a sulfonate anion (SO_3^-). It is one of the most widely used perfluorinated organic compounds. According to the European Food Safety Authority's Contaminants (CONTAM) Panel, food, in particular fish and fishery products, seem to be a significant source of exposure to these contaminants.[61] The mass spectrometric results from the samples during the redox reaction of PFOS with a typical TiO_2-based photocatalyst and its comparison to BEEP performance are presented in Fig. 5C and D. When only the photocatalysis was employed, almost no removal of PFOS occurred. When BEEP was applied, a decrease in the concentration of PFOS was observed and approximately 30 percent of the starting material was eradicated in 24 h. This indicates that the BEEP technology is capable of eliminating not only the longer chain PFAS compounds, but it can also effectively target the robust ions and molecules like PFOS and PFOA, the main pollutants in the PFAS family. Although the rates of removal of PFOS and PFOA are slower compared to the longer chain PFAS, BEEP technology is a promising alternative to other expensive and destructive methods such as electrolysis and supercritical water oxidation.

The released F^- ions were quantified by an ion-selective electrode (ISE, Mettler Toledo solid-state) connected to a Mettler Toledo SevenCompact pH/ion meter. The accuracy of F^- measurement by the ISE was validated by spiking various concentrations of NaF into the solution matrices. The

defluorination percentage is defined as the concentration ratio between the released F^- ions in solution and the total fluorine in the parent PFOS molecule. When only photocatalysis was applied the initial concentration of F^- was 0.001 ppm at the start and did not change after 24 h of redox reaction. In contrast, for the BEEP experiment, the initial PFOS sample showed 0.005 ppm fluoride ion concentration and at 24 h was 0.210 ppm, a defluorination percentage of approximately 15%. This defluorination ratio shows that an appreciable quantity of PFOS is completely mineralized to its components. A longer experiment was conducted, and it was observed that with an increase in time, the amount of free fluoride ions kept increasing. The amount of F^- observed for the initial sample was 0.004 ppm and for 1, 2, 4, 24, 48 and 72 h samples the readings were 0.012, 0.015, 0.018, 0.040, 0.068 and 0.087 ppm respectively. These results indicate that the BEEP is an effective *in situ* approach for the removal of forever chemicals in water. For the 72 h PFOS experiment, although a continuous increase in the fluoride concentration was observed, the mass spectrometric results indicated that after 24 h there was an increase in PFOS concentration (Fig. S8†). PFOS has a hydrophilic head and a hydrophobic fluorinated tail. Due to the long hydrophobic chain, PFOS has a high propensity for the surface where the hydrophobic end is sticking out of the water and the hydrophilic end is in the water. This phenomenon is the basis of the foam fractionation process for PFAS removal.[62] In BEEP, due to the vigorous water movement and wet scrubbing, a possible explanation is that a large number of PFOS molecules are present in the foam phase and travel to the photocatalyst surface area *via* the pump. As there is a 2V anodic voltage present on the photocatalyst, the hydrophilic head present on the water surface or in the microbubble gets attracted towards that positive charge and stays longer (Fig. 5B). The photocatalytic redox process defluorinates the ions. As more and more PFOS ions present on the surface were eliminated by BEEP, a significant decrease in the foam was observed during the 72 h experiment. The increase in the concentration of PFOS in 48 h and 72 h samples may be the result of PFOS ions previously sequestered in the foam being distributed into the solution phase.

Conclusions

We have developed an enhanced photocatalytic system where a TiO_2 nanoporous based photocatalyst is used in conjunction with a potential bias. Application of this bias significantly sequesters the electron–hole recombination and mitigates the effect of ionic interference during the photocatalytic process. The photoreactor was tested for the photocatalytic oxidation of rhodamine B to explore the reaction rates under different experimental conditions. Compared to a typical photocatalytic reactor, Bias Enhanced Electrolytic Photocatalysis (BEEP) performs about 50% faster in freshwater systems and an increase of 13%, 46%, 87%, and 640% in the photocatalytic performance was observed for 100, 1000, 3500 and 35 000 ppm salt solutions respectively. Where all the other photocatalytic systems become inefficient in the presence of salt and other inorganic minerals in the water, the BEEP-based photoreactor exhibits enhanced performance compared to the freshwater systems. The synergistic use of water scrubbing, laminar flow, and applied bias results in a significant enhancement in the photocatalytic efficiency of the photocatalytic system. As ionic interferences are limited in the BEEP photoreactor, testing was performed for the destruction of amphiphilic forever chemicals. To prove the photocatalytic capability of the reactor, a 537 M method was used where a mixture of 42 forever chemicals containing different functional groups such as carboxylic acid, sulphonic acid, sulphonamide, sulphonate, ether, *etc.*, was tested. The third-party testing revealed that BEEP could destroy most of the 42 forever chemicals, present in the water. The high-molecular-weight forever chemicals were most susceptible to degradation and within 24 h most of the compounds containing 10 or more carbon atoms in the molecular structure were undetectable by LC-MS/MS. Interestingly the concentration of compounds with a smaller carbon chain increased during the testing which reveals that the longer chains were being broken down into smaller chain species.

Employment of 365 nm UVA-LED also helps in decreasing the energy cost and significantly increasing the photocatalytic activity of the system. This LED-based technology is eco-friendly as it limits the use of harmful UVC lamps. As a portion of sunlight also contains UVA, these developed photoreactors in future can be employed in the sunlight thus fulfilling the goal of having a more energy-efficient wastewater treatment technology. This energy-efficient technology can be used equally in both freshwater and saltwater treatment and can remove organics, pathogens, and even forever chemicals from the wastewater. This significant enhancement in the BEEP photocatalysis can also be employed for other green chemistry applications.

Data availability

Data for this article, including raw data for all figures are available at Borealis > University of Victoria Dataverse Collection > Scott McIndoe Dataverse at **https://doi.org/10.5683/SP3/N050JU**.

Author contributions

The manuscript was written through the contributions of all authors. All authors have approved the final version of the manuscript. JBH and JSM initiated the project and supervised the study. SST developed the photocatalyst and performed the characterizations (SEM, XRD, EDX) and with BAR the photocatalysis studies. JSM, BAR, JBH, and MP developed the methodology. BAR, IC performed MS experimentation. BAR, JSM and IC helped in the interpretation of the MS data. SST wrote the original draft, which was reviewed and edited by BAR, JSM and JBH.

Conflicts of interest

JBH and SST are inventors on U.S. Provisional Patent Application US20230113314A1 & U.S. Patent US 11,919,786 B2, which claims the use of BEEP described in this work.

Acknowledgements

We thank the Centre for Advanced Materials and Related Technology (CAMTEC) at The University of Victoria for the SEM, EDX, and XRD analysis. Infrastructural and operational funding was provided by the Natural Sciences and Engineering Research Council of Canada and the New Frontiers in Research Fund.

Notes and references

1 B. Chen, M. Wang, M. Duan, X. Ma, J. Hong, F. Xie, R. Zhang and X. Li, In search of key: Protecting human health and the ecosystem from water pollution in China, *J. Clean. Prod.*, 2019, **228**, 101–111.

2 C. Zamora-Ledezma, D. Negrete-Bolagay, F. Figueroa, E. Zamora-Ledezma, M. Ni, F. Alexis and V. H. Guerrero, Heavy metal water pollution: A fresh look about hazards, novel and conventional remediation methods, *Environ. Technol. Innovat.*, 2021, **22**, 101504.

3 E. R. Jones, M. F. P. Bierkens, P. J. T. M. van Puijenbroek, L. P. H. van Beek, N. Wanders, E. H. Sutanudjaja and M. T. H. van Vliet, Sub-Saharan Africa will increasingly become the dominant hotspot of surface water pollution, *Nat. Water*, 2023, **1**, 602–613.

4 J. Cui, P. Gao and Y. Deng, Destruction of Per- and Polyfluoroalkyl Substances (PFAS) with Advanced Reduction Processes (ARPs): A Critical Review, *Environ. Sci. Technol.*, 2020, **54**, 3752–3766.

5 C. G. Scheitlin, K. Dasu, S. Rosansky, L. E. Dejarme, D. Siriwardena, J. Thorn, L. Mullins, I. Haggerty, K. Shqau and J. Stowe, Application of Supercritical Water Oxidation to Effectively Destroy Per- and Polyfluoroalkyl Substances in Aqueous Matrices, *ACS ES&T Water*, 2023, **3**, 2053–2062.

6 J. Li, C. Austin, S. Moore, B. R. Pinkard and I. V. Novosselov, PFOS destruction in a continuous supercritical water oxidation reactor, *Chem. Eng. J.*, 2023, **451**, 139063.

7 S. J. Smith, K. Wiberg, P. McCleaf and L. Ahrens, Pilot-Scale Continuous Foam Fractionation for the Removal of Per- and Polyfluoroalkyl Substances (PFAS) from Landfill Leachate, *ACS ES&T Water*, 2022, **2**, 841–851.

8 S. J. Smith, M. Lauria, L. Ahrens, P. McCleaf, P. Hollman, S. Bjälkefur Seroka, T. Hamers, H. P. H. Arp and K. Wiberg, Electrochemical Oxidation for Treatment of PFAS in Contaminated Water and Fractionated Foam – A Pilot-Scale Study, *ACS ES&T Water*, 2023, **3**, 1201–1211.

9 S. Dong, J. Feng, M. Fan, Y. Pi, L. Hu, X. Han, M. Liu, J. Sun and J. Sun, Recent developments in heterogeneous photocatalytic water treatment using visible light-responsive photocatalysts: a review, *RSC Adv.*, 2015, **5**, 14610–14630.

10 S. Pandey, K. K. Mandari, J. Kim, M. Kang and E. Fosso-Kankeu, in *Photocatalysts in Advanced Oxidation Processes for Wastewater Treatment*, 2020, pp. 167–196, DOI: **10.1002/9781119631422.ch6**.

11 Y. Nosaka and A. Y. Nosaka, Generation and Detection of Reactive Oxygen Species in Photocatalysis, *Chem. Rev.*, 2017, **117**, 11302–11336.

12 Y. Li, T.-X. Luan, K. Cheng, D. Zhang, W. Fan, P.-Z. Li and Y. Zhao, Effective Photocatalytic Initiation of Reactive Oxygen Species by a Photoactive Covalent Organic Framework for Oxidation Reactions, *ACS Mater. Lett.*, 2022, **4**, 1160–1167.

13 J. Schneider, M. Matsuoka, M. Takeuchi, J. Zhang, Y. Horiuchi, M. Anpo and D. W. Bahnemann, Understanding TiO_2 Photocatalysis: Mechanisms and Materials, *Chem. Rev.*, 2014, **114**, 9919–9986.

14 S. S. Thind, G. Wu and A. Chen, Synthesis of mesoporous nitrogen–tungsten co-doped TiO_2 photocatalysts with high visible light activity, *Appl. Catal. B Environ.*, 2012, **111–112**, 38–45.

15 A. Purabgola, N. Mayilswamy and B. Kandasubramanian, Graphene-based TiO_2 composites for photocatalysis & environmental remediation: synthesis and progress, *Environ. Sci. Pollut. Res.*, 2022, **29**, 32305–32325.

16 X. Chang, S. S. Thind and A. Chen, Electrocatalytic Enhancement of Salicylic Acid Oxidation at Electrochemically Reduced TiO_2 Nanotubes, *ACS Catal.*, 2014, **4**, 2616–2622.

17 K. Hu, R. Li, C. Ye, A. Wang, W. Wei, D. Hu, R. Qiu and K. Yan, Facile synthesis of Z-scheme composite of TiO_2 nanorod/g-C_3N_4 nanosheet efficient for photocatalytic degradation of ciprofloxacin, *J. Clean. Prod.*, 2020, **253**, 120055.

18 B. A. Marinho, S. M. A. G. U. de Souza, A. A. U. de Souza and D. Hotza, Electrospun TiO_2 nanofibers for water and wastewater treatment: a review, *J. Mater. Sci.*, 2021, **56**, 5428–5448.

19 E. Horváth, J. Gabathuler, G. Bourdiec, E. Vidal-Revel, M. Benthem Muñiz, M. Gaal, D. Grandjean, F. Breider, L. Rossi, A. Sienkiewicz and L. Forró, Solar water purification with photocatalytic nanocomposite filter based on TiO_2 nanowires and carbon nanotubes, *npj Clean Water*, 2022, **5**, 10.

20 K. Guo, B. Jiang, P. Zhao, Y. Wu, S. Tian, Z. Gao, L. Zong and S. Yao, Review on the Superhydrophilic coating of Electric insulator, *IOP Conf. Ser. Earth Environ. Sci.*, 2021, **651**, 022037.

21 M. Sansotera, F. Persico, C. Pirola, W. Navarrini, A. Di Michele and C. L. Bianchi, Decomposition of perfluorooctanoic acid photocatalyzed by titanium dioxide: chemical modification of the catalyst surface induced by fluoride ions, *Appl. Catal. B Environ.*, 2014, **148–149**, 29–35.

22 Z. Wang, M. Li, W. Cao, Z. Liu, D. Kong and W. Jiang, Efficient photocatalytic degradation of perfluorooctanoic acid by bismuth nanoparticle modified titanium dioxide, *Sci. Total Environ.*, 2024, **927**, 172028.

23 M.-J. Chen, S.-L. Lo, Y.-C. Lee, J. Kuo and C.-H. Wu, Decomposition of perfluorooctanoic acid by ultraviolet light irradiation with Pb-modified titanium dioxide, *J. Hazard. Mater.*, 2016, **303**, 111–118.

24 Z. Li, P. Zhang, T. Shao, J. Wang, L. Jin and X. Li, Different nanostructured In_2O_3 for photocatalytic decomposition of perfluorooctanoic acid (PFOA), *J. Hazard. Mater.*, 2013, **260**, 40–46.

25 M. Sansotera, F. Persico, C. Pirola, W. Navarrini, A. D. Michele and C. L. Bianchi, *Appl. Catal. B Environ.*, 2014, **148–149**, 29–35.

26 Z. U. Zango, K. S. Khoo, A. Garba, H. A. Kadir, F. Usman, M. U. Zango, W. Da Oh and J. W. Lim, A review on superior advanced oxidation and photocatalytic degradation techniques for perfluorooctanoic acid (PFOA) elimination from wastewater, *Environ. Res.*, 2023, **221**, 115326.

27 S. C. E. Leung, P. Shukla, D. Chen, E. Eftekhari, H. An, F. Zare, N. Ghasemi, D. Zhang, N.-T. Nguyen and Q. Li, Emerging technologies for PFOS/PFOA degradation and removal: a review, *Sci. Total Environ.*, 2022, **827**, 153669.

28 S. A. Younis and K.-H. Kim, *Heterogeneous Photocatalysis Scalability for Environmental Remediation: Opportunities and Challenges*, 2020, vol. 10, p. 1109.

29 S. K. Loeb, P. J. J. Alvarez, J. A. Brame, E. L. Cates, W. Choi, J. Crittenden, D. D. Dionysiou, Q. Li, G. Li-Puma, X. Quan, D. L. Sedlak, T. David Waite, P. Westerhoff and J.-H. Kim, The Technology Horizon for Photocatalytic Water Treatment: Sunrise or Sunset?, *Environ. Sci. Technol.*, 2019, **53**, 2937–2947.

30 H. Dong, G. Zeng, L. Tang, C. Fan, C. Zhang, X. He and Y. He, An overview on limitations of TiO_2-based particles for photocatalytic degradation of organic pollutants and the corresponding countermeasures, *Water Res.*, 2015, **79**, 128–146.

31 S. Peiris, H. B. de Silva, K. N. Ranasinghe, S. V. Bandara and I. R. Perera, *Recent Development and Future Prospects of TiO2 Photocatalysis*, 2021, vol. 68, pp. 738–769.

32 V. Likodimos, C. Han, M. Pelaez, A. G. Kontos, G. Liu, D. Zhu, S. Liao, A. A. de la Cruz, K. O'Shea, P. S. M. Dunlop, J. A. Byrne, D. D. Dionysiou and P. Falaras, Anion-Doped TiO_2 Nanocatalysts for Water Purification under Visible Light, *Ind. Eng. Chem. Res.*, 2013, **52**, 13957–13964.

33 S. Sun, J. Zhang, P. Gao, Y. Wang, X. Li, T. Wu, Y. Wang, Y. Chen and P. Yang, Full visible-light absorption of TiO_2 nanotubes induced by anionic S_2^{2-} doping and their greatly enhanced photocatalytic hydrogen production abilities, *Appl. Catal. B Environ.*, 2017, **206**, 168–174.

34 S. S. Thind, G. Wu, M. Tian and A. Chen, Significant enhancement in the photocatalytic activity of N, W co-doped TiO_2 nanomaterials for promising environmental applications, *Nanotechnology*, 2012, **23**, 475706.

35 S. Sood, A. Umar, S. K. Mehta and S. K. Kansal, Highly effective Fe-doped TiO_2 nanoparticles photocatalysts for visible-light driven photocatalytic degradation of toxic organic compounds, *J. Colloid Interface Sci.*, 2015, **450**, 213–223.

36 Y. Guo, P. Wang, J. Qian, J. Hou, Y. Ao and C. Wang, Construction of a composite photocatalyst with significantly enhanced photocatalytic performance through combination of homo-junction with hetero-junction, *Catal. Sci. Technol.*, 2018, **8**, 486–498.

37 M. Dahl, Y. Liu and Y. Yin, Composite Titanium Dioxide Nanomaterials, *Chem. Rev.*, 2014, **114**, 9853–9889.

38 H. Ren, J.-L. Yang, W.-M. Yang, H.-L. Zhong, J.-S. Lin, P. M. Radjenovic, L. Sun, H. Zhang, J. Xu, Z.-Q. Tian and J.-F. Li, Core–Shell–Satellite Plasmonic Photocatalyst for Broad-Spectrum Photocatalytic Water Splitting, *ACS Mater. Lett.*, 2021, **3**, 69–76.

39 W. Ren, R. Si, J. Wang, Y. Yang, X. Zheng and S. Chen, Study of the different morphologies of Zn0.5Cd0.5S for photocatalytic H_2 production, *Environ. Sci.: Adv.*, 2023, **2**, 721–730.

40 F. O. Ochedi, D. Liu, J. Yu, A. Hussain and Y. Liu, Photocatalytic, electrocatalytic and photoelectrocatalytic conversion of carbon dioxide: a review, *Environ. Chem. Lett.*, 2021, **19**, 941–967.

41 Y. Wang, M. Zu, X. Zhou, H. Lin, F. Peng and S. Zhang, Designing efficient TiO_2-based photoelectrocatalysis systems for chemical engineering and sensing, *Chem. Eng. J.*, 2020, **381**, 122605.

42 C. Dette, M. A. Pérez-Osorio, C. S. Kley, P. Punke, C. E. Patrick, P. Jacobson, F. Giustino, S. J. Jung and K. Kern, TiO_2 Anatase with a Bandgap in the Visible Region, *Nano Lett.*, 2014, **14**, 6533–6538.

43 A. N. Che Abdul Rahim, S. Yamada, H. Bonkohara, S. Mestre, T. Imai, Y.-T. Hung and I. Kumakiri, *Influence of Salts on the Photocatalytic Degradation of Formic Acid in Wastewater*, 2022, vol. 19, p. 15736.

44 C. Guillard, E. Puzenat, H. Lachheb, A. Houas and J.-M. Herrmann, Why inorganic salts decrease the TiO2 photocatalytic efficiency, *Int. J. Photoenergy*, 2005, **7**, 641208.

45 M. F. Rahman, S. Peldszus and W. B. Anderson, Behaviour and fate of perfluoroalkyl and polyfluoroalkyl substances (PFASs) in drinking water treatment: a review, *Water Res.*, 2014, **50**, 318–340.

46 J. Glüge, M. Scheringer, I. T. Cousins, J. C. DeWitt, G. Goldenman, D. Herzke, R. Lohmann, C. A. Ng, X. Trier and Z. Wang, An overview of the uses of per- and polyfluoroalkyl substances (PFAS), *Environ. Sci.: Processes Impacts*, 2020, **22**, 2345–2373.

47 E. M. Sunderland, X. C. Hu, C. Dassuncao, A. K. Tokranov, C. C. Wagner and J. G. Allen, A review of the pathways of human exposure to poly- and perfluoroalkyl substances (PFASs) and present understanding of health effects, *J. Expo. Sci. Environ. Epidemiol.*, 2019, **29**, 131–147.

48 E. M. Bell, S. De Guise, J. R. McCutcheon, Y. Lei, M. Levin, B. Li, J. F. Rusling, D. A. Lawrence, J. M. Cavallari, C. O'Connell, B. Javidi, X. Wang and H. Ryu, Exposure, health effects, sensing, and remediation of the emerging PFAS contaminants – scientific challenges and potential research directions, *Sci. Total Environ.*, 2021, **780**, 146399.

49 S. E. Fenton, A. Ducatman, A. Boobis, J. C. DeWitt, C. Lau, C. Ng, J. S. Smith and S. M. Roberts, *Per- and Polyfluoroalkyl Substance Toxicity and Human Health Review: Current State of Knowledge and Strategies for Informing Future Research*, 2021, vol. 40, pp. 606–630.

50 P. Grandjean, C. Heilmann, P. Weihe, F. Nielsen, U. B. Mogensen, A. Timmermann and E. Budtz-Jørgensen, Estimated exposures to perfluorinated compounds in infancy predict attenuated vaccine antibody concentrations at age 5-years, *J. Immunot.*, 2017, **14**, 188–195.

51 C. Looker, M. I. Luster, A. M. Calafat, V. J. Johnson, G. R. Burleson, F. G. Burleson and T. Fletcher, Influenza Vaccine Response in Adults Exposed to Perfluorooctanoate and Perfluorooctanesulfonate, *Toxicol. Sci.*, 2013, **138**, 76–88.

52 S. Verma, T. Lee, E. Sahle-Demessie, M. Ateia and M. N. Nadagouda, Recent advances on PFAS degradation via thermal and nonthermal methods, *Chem. Eng. J. Adv.*, 2023, **13**, 100421.

53 M. Kah, D. Oliver and R. Kookana, Sequestration and potential release of PFAS from spent engineered sorbents, *Sci. Total Environ.*, 2021, **765**, 142770.

54 M. Saleem, G. Tomei, M. Beria, E. Marotta and C. Paradisi, Highly efficient degradation of PFAS and other surfactants in water with atmospheric Radial plasma (RAP) discharge, *Chemosphere*, 2022, **307**, 135800.

55 B. Xu, M. B. Ahmed, J. L. Zhou, A. Altaee, M. Wu and G. Xu, Photocatalytic removal of perfluoroalkyl substances from water and wastewater: Mechanism, kinetics and controlling factors, *Chemosphere*, 2017, **189**, 717–729.

56 Y. Wen, Á. Rentería-Gómez, G. S. Day, M. F. Smith, T.-H. Yan, R. O. K. Ozdemir, O. Gutierrez, V. K. Sharma, X. Ma and H.-C. Zhou, Integrated Photocatalytic Reduction and Oxidation of Perfluorooctanoic Acid by Metal–Organic Frameworks: Key Insights into the Degradation Mechanisms, *J. Am. Chem. Soc.*, 2022, **144**, 11840–11850.

57 J. A. Shoemaker, P. Grimmett, B. Boutin, *Determination of Selected Perfluorinated Alkyl Acids in Drinking Water by Solid Phase Extraction and Liquid Chromatography/Tandem Mass Spectrometry (LC/MS/MS)*, U.S. Environmental Protection Agency, Washington, DC, 2008.

58 J. A. Shoemaker, D. Tettenhorst, *Method 537.1 Determination of Selected Per- and Polyflourinated Alkyl Substances in Drinking Water by Solid Phase Extraction and Liquid Chromatography/Tandem Mass Spectrometry (LC/MS/MS)*, US Environmental Protection Agency, Washington DC, 2020.

59 C. P. West, H. M. Brown and P. W. Fedick, Molecular Characterization of the Thermal Degradation of Per- and Polyfluoroalkyl Substances in Aqueous Film-Forming Foams via Temperature-Programmed Thermal Desorption–Pyrolysis–Direct Analysis in Real Time–Mass Spectrometry, *Environ. Sci. Technol. Lett.*, 2023, **10**, 308–315.

60 K. Park, I. Ali and J.-O. Kim, Photodegradation of perfluorooctanoic acid by graphene oxide-deposited TiO_2 nanotube arrays in aqueous phase, *J. Environ. Manage.*, 2018, **218**, 333–339.

61 E. F. S. Authority, *Perfluorooctane sulfonate (PFOS), perfluorooctanoic acid (PFOA) and their salts Scientific Opinion of the Panel on Contaminants in the Food chain*, 2008, vol. 6, p. 653.

62 S. J. Smith, J. Lewis, K. Wiberg, E. Wall and L. Ahrens, Foam fractionation for removal of per- and polyfluoroalkyl substances: towards closing the mass balance, *Sci. Total Environ.*, 2023, **871**, 162050.